Fault Detection using Data-driven LPV State Estimation based on Structural Analysis and ANFIS

Xin Fang[1], Joaquim Blesa[1,2] and Vicenç Puig[1]

Abstract— This paper presents a data-driven fault detection method combining structural analysis (SA) and machine learning data-driven algorithms. Given a graphic (or textual) system description and the available inputs/outputs measurements, the structure of analytical redundancy relations (ARRs) between some inputs and outputs can be determined with the aid of the SA of the system. Then, using a machine learning data-driven approach applied to historical data, analytical relations between inputs and outputs can be obtained. Thereby, instead of finding ARRs from physical mathematical model, ARRs are obtained combining SA and data-driven approaches. In this paper, the adaptive network fuzzy inference system (ANFIS) data-driven approach is used to implement the diagnosis system. Once the ANFIS model has been identified, it is reformulated in linear parameter varying (LPV) form. Then, a fault detection scheme based on a LPV Kalman filter and pole placement method is developed. A well-known case study based on a four-tanks system is used for illustrative purposes.

I. INTRODUCTION

The diagnosis of complex industrial systems has always been an important feature to consider in industrial technical context. In any industrial system, the occurrence of faults may cause unfavorable consequences of different degree, from temporary interruption of the system to permanent paralysis. Thereby, in-time correct detection of faults can reduce significantly possible losses to these systems. Fault diagnosis has been studied during long time by investigators from different communities, mainly from automatic control and artificial intelligence ones [1]. Both communities have developed their own diagnosis approaches: the FDI (Fault Detection and Isolation) approaches, based on engineering disciplines, such as control theory and statistical decision making and the DX (Diagnosis) approaches, based on the fields of logic, combinatorial optimization, search and complexity analysis. In the last years, some fault diagnosis methodologies have been developed taking profit from both FDI and DX approaches [2]. Both approaches require quantitative of qualitative models of the system to carry out the fault diagnosis. The basic model-based fault diagnosis approach consist in comparing the observed behaviour of the system to its expected behaviour given by the model prediction. This comparison can be carried out by means the computation of a residual resulting from the difference of a process measured variable and its estimation provided by a model. Ideally, residuals must be zero to guarantee the correct functionality of the system but there are always external disturbances and modelling inaccuracy that make residuals deviate from zero even in a fault-free scenario. So, model uncertainty has to be taken into account in the fault detection stage for example by means of the computation of a threshold that takes into account the maximum value of model uncertainties. The determination of the threshold to distinguish true faults from irrelevant signal fluctuating is a key point in the performance of the fault detection. The election of this threshold is a trade-off between the proportion of times that the detection is activated in a fault free scenario or false alarm rate (FAR) and the proportion of detected faults or fault detection rate (FDR) [3]. So, it is crucial to obtain a mathematical model as exact as possible to describe the system to be monitored. But, the availability of an accurate model is complicated in some complex industrial systems. As mentioned in [4], to overcome the difficulty of obtaining a mathematical model of a system which is required for the majority of current diagnosis methods, instead of finding the exact physical equations of the system, methods that only require structural ARRs (Analytical Redundancy Relations) of the system obtained by means of Structural Analysis (SA) and data are reviewed in [5].

This paper presents a data-driven fault detection method combining structural analysis (SA) and machine learning data-driven algorithms. Given a graphic (or textual) system description and the available inputs/outputs measurements, the structure of analytical redundancy relations (ARRs) between some inputs and outputs can be determined with the aid of system SA. Then, applying a machine learning data-driven approach (for example, the so-called adaptive network fuzzy inference system (ANFIS) [6]) to historical data, analytical expressions between inputs and outputs can be obtained. Thereby, instead of finding ARRs from physical mathematical model, combining SA and ANFIS using historical data, a set of data-driven ARRs can be obtained and used to implement a diagnosis system. Once the ANFIS model has been identified, it is reformulated in linear parameter varying (LPV) form. Then, a fault detection scheme based on a LPV Kalman filter and pole placement method is developed. A well-known case study based on a four-tank system is used for illustrative purposes.

The paper has the following structure: Section II presents the general problem statement, and it is followed by the Section III where state estimation is developed. In Section IV, a case study of four tanks is introduced to show the practical

[1]Xin Fang, Joaquim Blesa and Vicenç Puig are with Institut de Robòtica i Informàtica Industrial, CSIC-UPC, Llorens i Artigas 4-6, 08028 Barcelona, Spain. and Supervision, Safety and Automatic Control Research Center (CS2AC) of the Universitat Politècnica de Catalunya, Rambla Sant Nebridi 22, 08222 Terrassa, Spain xin.fan@upc.edu, joaquim.blesa@upc.edu, vicenc.puig@upc.edu

[2] Joaquim Blesa is a Serra Húnter Fellow, UPC, Automatic Control Department (ESAII), Eduard Maristany 16, 08019 Barcelona, Spain
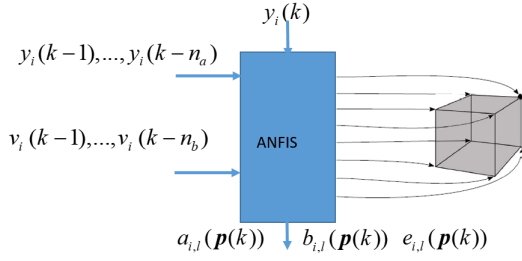
Fig. 1. ANFIS training with inputs

application of the proposed method. Finally, Section V draws the conclusions of the present paper.

II. PROBLEM STATEMENT

Given a system with measured inputs $\boldsymbol{u} \in \Re^{n_u}$ and outputs $\boldsymbol{y} \in \Re^{n_y}$. Using structural analysis [7], an ARR structure can be determined relating system inputs and outputs without having the physical mathematical model:

$$\hat{y}_i(k) = f_i(y_i(k-1), ..., y_i(k-n_a), \boldsymbol{y}_{\neg i(k-1)}, ...$$
$$..., \boldsymbol{y}_{\neg i(k-n_a)}, \boldsymbol{u}_i(k-1), , ..., \boldsymbol{u}_i(k-n_a))$$
$$i = 1, ..., n_y \quad (1)$$

where $\hat{y}_i(k) \in \Re$ represents the estimation of the i-th component of $\boldsymbol{y}$ at instant k, $f_i()$ is an unknown complex function of order n_a. Without any structural analysis

$$\boldsymbol{y}_{\neg i}(k-j) = \boldsymbol{y}(k-j) \backslash y_i(k-j) \quad j = 1, ..., n_a \quad (2)$$

$$\boldsymbol{u}_i(k-j) = \boldsymbol{u}(k-j) \quad j = 1, ..., n_a \quad (3)$$

but if structural analysis is available, the number of components of $\boldsymbol{y}_{\neg i}(k-j)$ and $\boldsymbol{u}_i(k-j)$ could decrease. Defining

$$\boldsymbol{v}_i(k-j) = (\boldsymbol{y}_{\neg i}(k-j) \quad \boldsymbol{u}_i(k-j)) \quad j = 1, ..., n_a$$

equation (1) can be rewritten as

$$\hat{y}_i(k) = f_i(y_i(k-1), ..., y_i(k-n_a), \boldsymbol{v}_i(k-1), ...$$
$$..., \boldsymbol{v}_i(k-n_a)) \quad (4)$$
$$i = 1, ..., n_y$$

The consistency of model (4) and the actual behaviour of the system can be assessed by means the difference (residual) of the actual output $y_i(k)$ and its estimation

$$r_i(k) = y_i(k) - \hat{y}_i(k) \quad i = 1, ..., n_y \quad (5)$$

In a fault-free scenario, residuals $r_i(k)$ are different from zero because of modelling errors and noise. If enough fault-free data is available a threshold σ_i can be computed as the maximum observed error and used for fault detection purposes as

$$\begin{cases} r_i(k) \leq \sigma_i \Rightarrow \text{ No Fault} \\ r_i(k) > \sigma_i \Rightarrow \text{ Fault} \end{cases} \quad (6)$$

Model (4) can be fit considering non-faulty historical data and assuming linearity or some kind of non-linearity in

function $f_i()$ using computational tools [8] or using other parameter estimation techniques.

In artificial intelligence community, there are two main parameter estimation techniques, which are fuzzy logic and artificial neural network. Regarding to fuzzy logic, any member is included in a cluster with different membership degrees. An artificial neural network is a method of learning with samples, it is formed by artificial neurons. Lately, the adaptive network fuzzy inference system (ANFIS) hybrid method was proposed which is a combination of the two mentioned techniques above. In ANFIS, the advantages from both techniques are combined: learning ability and relational structure of the artificial neural networks and decision-making mechanism of the fuzzy logic [9].

ANFIS training approaches contain two different parameter groups: premise and consequence. The determination of these parameters is carried out by some predefined optimization algorithms, which will affect the approach performance, so the selection of optimization algorithm is an important feature to consider.

Using ANFIS and the structure of model (4), the model can be formulated as the following LPV-IO form:

$$\hat{y}_i(k) = -\sum_{l=1}^{n_a} a_{i,l}(\boldsymbol{p}_i(k)) y_i(k-l) + \sum_{l=1}^{n_a} \boldsymbol{b}_{i,l}(\boldsymbol{p}_i(k)) \boldsymbol{v}_i(k-l)$$
$$+ e_i(\boldsymbol{p}_i(k)) \quad (7)$$

where

$$a_{i,l}(\boldsymbol{p}_i(k)) = \sum_{j=1}^{Nv} \mu_i^j(\boldsymbol{p}_i(k)) a_{i,l}^j$$

$$\boldsymbol{b}_{i,l}(\boldsymbol{p}_i(k)) = \sum_{j=1}^{Nv} \mu_i^j(\boldsymbol{p}_i(k)) b_{i,l}^j$$

$$e_i(\boldsymbol{p}_i(k)) = \sum_{j=1}^{Nv} \mu_i^j(\boldsymbol{p}_i(k)) e_i^j$$

$$\boldsymbol{p}_i(k) = (y_i(k-1), ..., y_i(k-n_a), \boldsymbol{v}_i(k-1), ..., \boldsymbol{v}_i(k-n_a))$$

with Nv equal to $m_f{}^{n_u}$ where m_f and n_u represent the number of branch in the fuzzification layer of ANFIS structure and input variables number, respectively.

Therefore, the system in LPV-IO form can be rewritten in the following state-space (SS) representation:

$$\hat{\boldsymbol{x}}_i(k+1) = \boldsymbol{A}_i(\boldsymbol{p}_i(k)) \hat{\boldsymbol{x}}_i(k) + \boldsymbol{B}_i(\boldsymbol{p}_i(k)) \boldsymbol{v}_i(k) \quad (8)$$
$$\hat{y}_i(k) = \boldsymbol{C}_i \hat{\boldsymbol{x}}_i(k) + e_i(\boldsymbol{p}_i(k)) \quad (9)$$

where

$$\boldsymbol{A}_i(\boldsymbol{p}_i(k)) = \begin{pmatrix} 0 & 0 & \cdots & 0 & -a_{i,1}(\boldsymbol{p}_i(k)) \\ 1 & 0 & \cdots & \cdots & -a_{i,2}(\boldsymbol{p}_i(k)) \\ 0 & \ddots & \ddots & \ddots & \vdots \\ \vdots & \ddots & \ddots & 0 & -a_{i,n_a-1}(\boldsymbol{p}(k)) \\ 0 & \cdots & 0 & 1 & -a_{i,n_a}(\boldsymbol{p}_i(k)) \end{pmatrix} \quad (10)$$

$$\boldsymbol{B}_i(\boldsymbol{p}_i(k)) = \begin{pmatrix} b_{i,1}(\boldsymbol{p}_i(k)) \\ b_{i,2}(\boldsymbol{p}_i(k)) \\ \vdots \\ b_{i,na-1}(\boldsymbol{p}_i(k)) \\ b_{i,na}(\boldsymbol{p}_i(k)) \end{pmatrix} \quad (11)$$

$$C_i = \begin{pmatrix} 0 & 0 & \cdots & 0 & 1 \end{pmatrix} \quad (12)$$

$$\boldsymbol{x}_i(k) = \begin{pmatrix} y_i(k) \\ y_i(k-1) \\ \vdots \\ y_i(k-n_a+1) \\ y_i(k-n_a) \end{pmatrix} \quad (13)$$

Matrices $\boldsymbol{A}_i$ and $\boldsymbol{B}_i$ of LPV model (8) can be expressed as a polytopic interpolation of vertex $\boldsymbol{A}_i^j$ and $\boldsymbol{B}_i^j$ $j = 1, ..., N_v$ are that in the case of $\boldsymbol{A}_i^j$ the vertex are defined as

$$\boldsymbol{A}_i^j = \begin{pmatrix} 0 & 0 & \cdots & 0 & -\mu_i^j(\boldsymbol{p}_i(k))a_{i,1}^j \\ 1 & 0 & \cdots & \cdots & -\mu_i^j(\boldsymbol{p}_i(k))a_{i,2}^j \\ 0 & \ddots & \ddots & \ddots & \vdots \\ \vdots & \ddots & \ddots & 0 & -\mu_i^j(\boldsymbol{p}_i(k))a_{i,n_a-1}^j \\ 0 & \cdots & 0 & 1 & -\mu_i^j(\boldsymbol{p}_i(k))a_{i,n_a}^j \end{pmatrix} \quad (14)$$

III. LPV STATE ESTIMATION

According to [10], an autoregressive-moving average (ARMA) residual can be obtained applying the estimation provided by (8) in (5). ARMA residuals present some problems with error models, disturbances and error noises and usually are formulated as Luenberger observers [11] that add a proportional feedback of the error to the state estimation. As in the case of (8) matrix $\boldsymbol{A}_i$ depends on $\boldsymbol{p}_i(k)$, proportional gain matrix $\boldsymbol{L}_i$ will also depend on $\boldsymbol{p}_i(k)$ and the output estimation will be given by

$$\hat{\boldsymbol{x}}_i(k+1) = \boldsymbol{A}_i(\boldsymbol{p}_i(k))\hat{\boldsymbol{x}}_i(k) + \boldsymbol{B}_i(\boldsymbol{p}_i(k))\boldsymbol{v}_i(k)$$
$$+ \boldsymbol{L}_i(\boldsymbol{p}_i(k))(y_i(k) - \hat{y}_i(k)) \quad (15)$$

$$\hat{y}_i(k) = \boldsymbol{C}_i\hat{\boldsymbol{x}}_i(k) + e_i(\boldsymbol{p}_i(k)) \quad (16)$$

with $\boldsymbol{L}_i(\boldsymbol{p}_i(k))$ expressed in polytopic form as

$$\boldsymbol{L}_i(\boldsymbol{p}_i(k)) = \sum_{j=1}^{Nv} \mu_i^j(\boldsymbol{p}_i(k))\boldsymbol{L}_i^j \quad (17)$$

where $\boldsymbol{L}_i^j$ $j = 1, .., n_v$ are the vertex of $\boldsymbol{L}_i(\boldsymbol{p}_i(k))$.

In present paper, two observer-design methods will be used: Kalman filter and Pole placement methods.

A. Kalman filter

Kalman filter computes the optimal estimation when the system is affected by state disturbance and process noise denoted as $\mathbf{w}(k)$ and $n(k)$ in the following equation

$$\boldsymbol{x}_i(k+1) = \boldsymbol{A}_i(\boldsymbol{p}_i(k))\hat{\boldsymbol{x}}_i(k) + \boldsymbol{B}_i(\boldsymbol{p}_i(k))\boldsymbol{v}_i(k) + \mathbf{w}(k) \quad (18)$$
$$y_i(k) = \boldsymbol{C}_i\hat{\boldsymbol{x}}_i(k) + e_i(\boldsymbol{p}_i(k)) + n(k) \quad (19)$$

The gain of Kalman filter is computed in the following way:

$$\boldsymbol{L}_i^j = \boldsymbol{W}_i^j\boldsymbol{Y} \quad j = 1, .., N_v \quad (20)$$

with $\boldsymbol{W}^j$ and $\boldsymbol{Y}$ obtained by means the LMI:

$$\begin{pmatrix} \gamma I_{n_a} & I_{n_a} \\ I_{n_a} & \boldsymbol{Y} \end{pmatrix} > 0 \quad (21)$$

$$\begin{pmatrix} -\boldsymbol{Y} & \boldsymbol{Y}\boldsymbol{A}_i^{j'} - \boldsymbol{W}^{j'}\boldsymbol{C}_i' & \boldsymbol{Y}\boldsymbol{H}' & \boldsymbol{W}^{j'} \\ \boldsymbol{A}_i^j\boldsymbol{Y} - \boldsymbol{C}_i\boldsymbol{W}^j & -\boldsymbol{Y} & 0 & 0 \\ \boldsymbol{H}_i\boldsymbol{Y} & 0 & -1 & 0 \\ \boldsymbol{W}^j & 0 & 0 & -\boldsymbol{R}_i^{-1} \end{pmatrix} < 0 \quad (22)$$

where I_{n_a} is the identity matrix of n_a order, $\boldsymbol{R}_i$ and $\boldsymbol{H}_i$ take into account the disturbance and process noise bounds.

B. Pole placement

Another observer-design method is the pole placement approach that considers the poles of the system and with the observer matrix gain place the poles to a given region of the complex plane in order to accomplish some specific performance in state estimation (15).

$$\boldsymbol{L}_i^j = -\boldsymbol{W}^j\boldsymbol{P}^{-1} \quad j = 1, .., N_v \quad (23)$$

with $\boldsymbol{W}^j$ and $\boldsymbol{P}$ computed as follows

$$\boldsymbol{P} > 0 \quad (24)$$

$$\boldsymbol{P}\boldsymbol{A}_i^j - \boldsymbol{W}^j\boldsymbol{C}_i + (\boldsymbol{P}\boldsymbol{A}_i^j - \boldsymbol{W}^j\boldsymbol{C}_i)^T + 2\alpha_1\boldsymbol{P} < 0$$
$$\boldsymbol{P}\boldsymbol{A}_i^j - \boldsymbol{W}^j\boldsymbol{C}_i + (\boldsymbol{P}\boldsymbol{A}_i^j - \boldsymbol{W}^j\boldsymbol{C}_i)^T + 2\alpha_2\boldsymbol{P} > 0 \quad (25)$$

where α_1 and α_2 define the vertical band of LMI region. Their values are determined considering poles of general state estimation (15).

C. Fault detection strategy

Once both observers described above have been designed, residuals $r_{i1}(k)$ and $r_{i2}(k)$ can be computed applying the estimation provided by (15) in (5) considering $\boldsymbol{L}_i(\boldsymbol{p}_i(k))$ with observer gains $\boldsymbol{L}_i^j$ $j = 1, .., N_v$ in (17) computed following the Kalman approach $(r_{i1}(k))$ and pole placement approach $(r_{i2}(k))$. As in a fault free scenario in the presence only of model error and sensor noises, the Kalman filter should provide the optimal estimation, $r_{i1}(k)$ can be used as in (6) considering a threshold σ_{i1} computed as the maximum observed error by the Kalman observer with fault free data. Once that a fault has been detected, as not only model errors and sensor noises are present in the system Kalman observer loose the optimality. Then, $r_{i2}(k)$ can be used in (6) considering a threshold σ_{i2} computed as the maximum observed error by the Pole placement observer.

IV. APPLICATION EXAMPLE: FOUR-TANKS SYSTEM

The four-tanks process proposed in [12] and that was used in [13] for fault diagnosis purposes will illustrate the effectiveness of the method proposed in this paper. The inputs are u_1 and u_2 (input voltages to the two pumps) and

the outputs y_1, y_2, y_3 and y_4 (levels of the four tanks). Inputs and outputs are related by physical equations

$$\begin{aligned}
y_1(k) &= y_1(k-1) - \frac{a_1}{A_1}\sqrt{2gy_1(k-1)} + \\
&\quad \frac{a_3}{A_1}\sqrt{2gy_3(k-1)} + \frac{\gamma_1 k_1}{A_1}u_1(k-1) \\
y_2(k) &= y_2(k-1) - \frac{a_2}{A_2}\sqrt{2gy_2(k-1)} + \\
&\quad \frac{a_4}{A_2}\sqrt{2gy_4(k-1)} + \frac{\gamma_2 k_2}{A_2}u_2(k-1) \\
y_3(k) &= y_3(k-1) - \frac{a_3}{A_3}\sqrt{2gy_3(k-1)} + \\
&\quad \frac{(1-\gamma_2)k_2}{A_4}u_2(k-1) \\
y_4(k) &= y_4(k-1) - \frac{a_4}{A_4}\sqrt{2gy_4(k-1)} + \\
&\quad \frac{(1-\gamma_1)k_1}{A_4}u_1(k-1)
\end{aligned} \quad (26)$$

Considering only input/output information of the four-tank system and assuming first order function f_i, the four outputs and two inputs can be used in a model (4) that for the particular case will be

$$\hat{y}_i(k) = f_i(y_i(k-1), \boldsymbol{v}_i(k-1)) \quad i = 1, ..., 4 \quad (27)$$

where

$$\boldsymbol{v}_i(k-1) = (\boldsymbol{y}_{\neg i}(k-1) \quad u_1(k-1) \quad u_2(k-1)) \, i = 1, ..., 4 \quad (28)$$

However, by means structural analysis of the system and in particular using Minimal Structurally Over-determined (MSO) set approach (see [7] for more details), the following set of ARRs are obtained:

$$\begin{aligned}
\hat{y}_1(k) &= f_1(y_1(k-1), y_3(k-1), u_1(k-1)) \\
\hat{y}_2(k) &= f_2(y_2(k-1), y_4(k-1), u_1(k-1)) \\
\hat{y}_3(k) &= f_3(y_3(k-1), u_2(k-1)) \\
\hat{y}_4(k) &= f_4(y_4(k-1), u_1(k-1))
\end{aligned} \quad (29)$$

The number of parameters in these last equations is significantly less than in (27). For example, if we focus on $\hat{y}_3(k)$ computed in (27) with $\boldsymbol{v}_3(k-1)$ defined in (28) with five components: $y_1(k-1), y_2(k-1), y_4(k-1), u_1(k-1)$ and $u_2(k-1)$. With the structural analysis, $\hat{y}_3(k)$ is computed in (29) with $\boldsymbol{v}_3(k-1) = u_2(k-1)$, i.e, with only one component.

Then, by means of ANFIS method using available fault free historical data, considering minimal branches in fuzzification layer ($m_f = 2$) and input variable number ($n_u = 2$), the following LPV-IO model is obtained:

$$\hat{y}_3(k) = -\left(\sum_{j=1}^{4}(\mu_3^j(\boldsymbol{p}_3(k))a_3^j)\right)y_3(k-1) +$$

$$\left(\sum_{j=1}^{4}(\mu_3^j(\boldsymbol{p}_3(k))b_3^j)\right)u_2(k-1) + \left(\sum_{j=1}^{4}(\mu_3^j(\boldsymbol{p}_3(k))e_3^j)\right) \quad (30)$$

where

$$\boldsymbol{p}_3(k) = (y_3(k-1) \quad u_2(k-1)). \quad (31)$$

Thereby, the LPV-IO form shown before can be rewritten as SS form as follows:

$$\hat{\boldsymbol{x}}_3(k+1) = \boldsymbol{A}_3(\boldsymbol{p}_3(k))\hat{\boldsymbol{x}}_3(k) + \boldsymbol{B}_3(\boldsymbol{p}_3(k))\boldsymbol{v}_3(k) \quad (32)$$

$$\hat{y}_3(k) = \boldsymbol{C}_3\hat{\boldsymbol{x}}_3(k) + e_3(\boldsymbol{p}_3(k)) \quad (33)$$

where

$$\boldsymbol{A}_3(\boldsymbol{p}_3(k)) = -a_{3,1}(\boldsymbol{p}_3(k)) \quad (34)$$

$$\boldsymbol{B}_3(\boldsymbol{p}_3(k)) = b_{3,1}(\boldsymbol{p}_3(k)) \quad (35)$$

$$\boldsymbol{C}_3 = 1 \quad (36)$$

$$\boldsymbol{x}_3(k) = y_3(k) \quad (37)$$

In the same way, the LPV-IO state space model of $\hat{y}_1(k)$ can be obtained:

$$\hat{y}_1(k) = -\left(\sum_{j=1}^{8}(\mu_1^j(\boldsymbol{p}_1(k))a_1^j)\right)y_1(k-1) +$$

$$\left(\sum_{j=1}^{8}(\mu_3^j(\boldsymbol{p}_1(k))\boldsymbol{b}_1^j)\right)\left(\begin{array}{c} y_4(k-1) \\ u_2(k-1) \end{array}\right) \quad (38)$$

$$+ \left(\sum_{j=1}^{8}(\mu_1^j(\boldsymbol{p}_1(k))e_1^j)\right)$$

$$\hat{\boldsymbol{x}}_1(k+1) = \boldsymbol{A}_1(\boldsymbol{p}_1(k))\hat{\boldsymbol{x}}_1(k) + \boldsymbol{B}_1(\boldsymbol{p}_1(k))\boldsymbol{v}_1(k) \quad (39)$$

$$\hat{y}_1(k) = \boldsymbol{C}_1\hat{\boldsymbol{x}}_1(k) + e_1(\boldsymbol{p}_1(k)) \quad (40)$$

where

$$\boldsymbol{A}_1(\boldsymbol{p}_1(k)) = -a_{1,1}(\boldsymbol{p}_1(k)) \quad (41)$$

$$\boldsymbol{B}_1(\boldsymbol{p}_1(k)) = b_{1,1}(\boldsymbol{p}_1(k)) \quad (42)$$

$$\boldsymbol{C}_1 = 1 \quad (43)$$

$$\boldsymbol{x}_1(k) = y_1(k) \quad (44)$$

Finally, the other two LPV-IO state space models ($\hat{y}_2(k)$ and $\hat{y}_4(k)$) can be acquired analogously.

Once the system is represented in SS form, the diagnosis of itself can be developed. In particular, the Kalman filter and Pole placement observers are designed for the four outputs and thresholds σ_{i1} and σ_{i2} are computed as the maximum errors provided by the observers using fault free data. Then, fault detection can be applied as described in Section III. Some results are shown in the following.

As it is shown in Figures 2 and 3, in a fault-free scenario, the real level evolution of system (black color curve) is well-fitted with the estimation of Kalman filter observer (green color curve) which can prove the excellent performance of the Kalman filter observer in the case without presence of any fault. Then the corresponding residual evolution is also presented in both figures. Figures 4 and 5 and the upper part of Figures 6 and 7 show the same variables (tank levels, Kalman estimations and residuals considering Kalman approximation) when a sensor output fault of 4cm magnitude appears at $t = 200s$. As it can be observed in upper part of Figures 6 and 7, after the fault is detected using (6) appears what is known as "fault following effect" [11] and the fault is only detected for a short period of time. This problem is solved by means the strategy of the commutation of the use of the Kalman residual to the Pole placement residual when
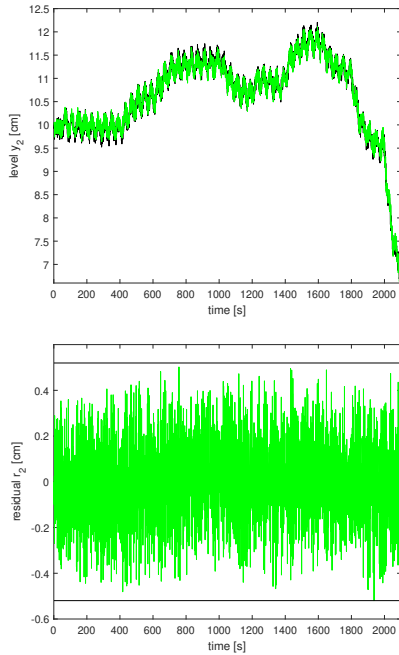
Fig. 2. Up: Tank 2 level $(y_2(k))$ in a fault-free scenario with Kalman estimation in green and real output in black. Down: Residual $r_{22}(k)$ and bounds defined by threshold σ_{22}
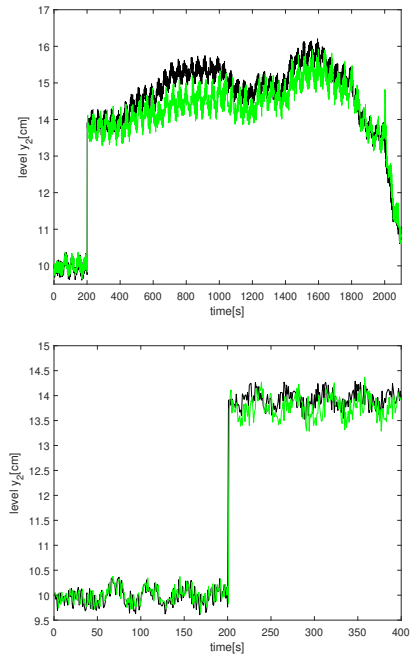
Fig. 4. Up: Tank 2 level $(y_2(k))$ in a sensor fault scenario at $t = 200s$ Kalman estimation of green and real output in black. Down: Detail around fault time
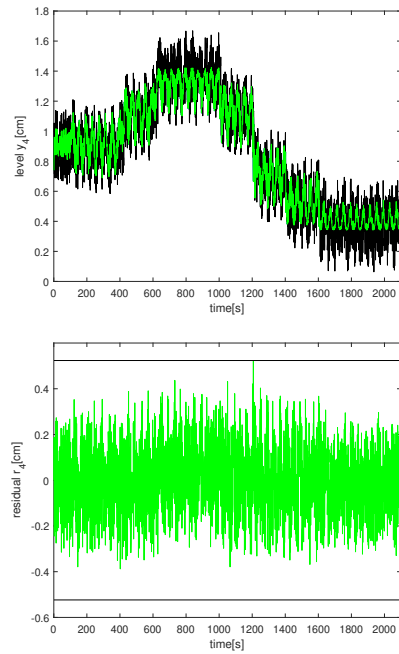
Fig. 3. Up: Tank 4 level $(y_4(k))$ in a fault-free scenario with Kalman estimation in green and real output in black. Down: Residual $r_{42}(k)$ and bounds defined by threshold σ_{42}
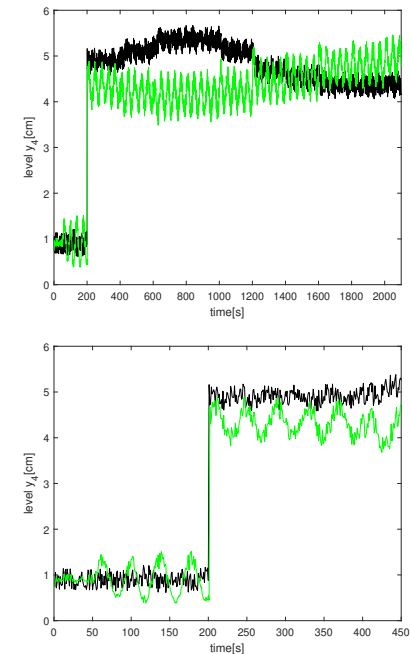
Fig. 5. Up: Tank 4 level $(y_4(k))$ in a sensor fault scenario at $t = 200s$ Kalman estimation of green and real output in black. Down: Detail around fault time
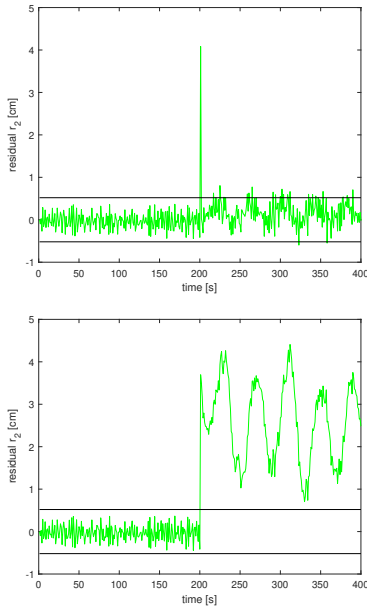
Fig. 6. Up: Tank 2 level residual ($r_2(k)$) in sensor fault scenario using Kalman estimation. Down: $r_2(k)$ in the same scenario but using Kalman estimation until fault detection time and Pole placement observer afterwards
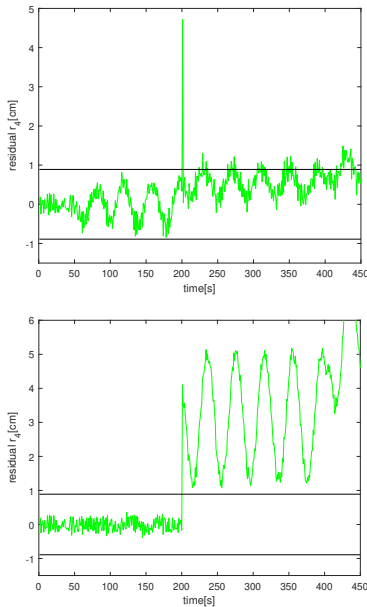
Fig. 7. Up: Tank 4 level residual ($r_4(k)$) in sensor fault scenario using Kalman estimation. Down: $r_4(k)$ in the same scenario but using Kalman estimation until fault detection time and Pole placement observer afterwards

a fault is detected as it is shown in the lower part of Figures 6 and 7. In this case, the fault alarm remains the excellent fitting with real output before fault occurs and once inside fault scenario, the fault alarm remains activated over time.

V. CONCLUSION

The present paper proposes an approach which combines SA and ANFIS to develop the fault diagnosis of complex systems. As result, the exact model of system is no longer indispensable, instead the structural information is needed which can be extracted from the given system description in order to acquire the corresponding structural ARRs. Afterwards, these ARRs can be transformed into analytical ARRs with aid of ANFIS using available historical data. As mentioned in Section III.C, this approach combines Kalman filter and Pole placement method to develop the estimation of model in the scenario with presence of fault. A four-tanks example has been used to show the performance of the proposed approach. The fault-following effect can be observed using only Kalman filter and the incorporation of Pole placement method has improved the performance of fault detection. The considered faults correspond to sensor faults of the 4 obtained ARRs which are the most critical faults in this context.

REFERENCES

[1] T. Escobet, A. Bregon, B. Pulido, V. Puig, Fault diagnosis of dynamic systems, Springer, 2019.
[2] L. Travé-Massuyès, Bridging control and artificial intelligence theories for diagnosis: A survey, Engineering Applications of Artificial Intelligence 27 (2014) 1–16.
[3] S. X. Ding, Model-based fault diagnosis techniques: design schemes, algorithms, and tools, Springer Science & Business Media, 2008.
[4] X. Fang, V. Puig, S. Zhang, Fault diagnosis and prognosis using a hybrid approach combining structural analysis and data-driven techniques, in: 2021 5th International Conference on Control and Fault-Tolerant Systems (SysTol), IEEE, 2021, pp. 145–150.
[5] L. Goupil, E. Chanthery, L. Travé-Massuyès, S. Delautier, A survey on diagnosis methods combining dynamic systems structural analysis and machine learning, in: 33rd International Workshop on Principle of Diagnosis–DX 2022, 2022.
[6] D. Karaboga, E. Kaya, Adaptive network based fuzzy inference system (anfis) training approaches: a comprehensive survey, Artificial Intelligence Review 52 (4) (2019) 2263–2293.
[7] M. Blanke, M. Kinnaert, J. Lunze, M. Staroswiecki, J. Schröder, Diagnosis and fault-tolerant control, Vol. 2, Springer, 2006.
[8] L. Ljung, System identification, in: Signal analysis and prediction, Springer, 1998, pp. 163–173.
[9] J.-S. Jang, Anfis: adaptive-network-based fuzzy inference system, IEEE transactions on systems, man, and cybernetics 23 (3) (1993) 665–685.
[10] J. Gertler, Fault detection and diagnosis in engineering systems, marcel and dekker, new york, ny, Search in (1998).
[11] V. Puig, J. Quevedo, T. Escobet, F. Nejjari, S. de las Heras, Passive robust fault detection of dynamic processes using interval models, IEEE Transactions on Control Systems Technology 16 (5) (2008) 1083–1089.
[12] K. H. Johansson, The quadruple-tank process: A multivariable laboratory process with an adjustable zero, IEEE Transactions on control systems technology 8 (3) (2000) 456–465.
[13] J. Blesa, V. Puig, J. Saludes, Robust identification and fault diagnosis based on uncertain multiple input–multiple output linear parameter varying parity equations and zonotopes, Journal of Process Control 22 (10) (2012) 1890–1912.